DSC-Vol. 55-2, Dynamic Systems and Control:
Volume 2
ASME 1994

A HIGH PRECISION TORQUE CONTROL OF A SELF MAGNETICALLY-LEVITATED SIX-DEGREE-OF-FREEDOM VARIABLE-RELUCTANCE SPHERICAL MOTOR

Zhi Zhou and Kok-Meng Lee
George W. Woodruff School of Mechanical Engineering
Georgia Institute of Technology
Atlanta, Georgia

ABSTRACT

Recent advances in manufacturing automation have motivated a flurry of research on multi-degree-of-freedom actuators. Among the development is a variable reluctance (VR) spherical motor which has potentials as a direct-drive robotic wrist capable of combining roll, yaw, and pitch motions in a single joint. Prior research on torque modeling of the VR spherical motor has shown that bearing friction due to the non-zero resultant magnetic force and loading contributes to the torque error, results in significant reactions on the transfer bearings, and generates high frequency noise. For this reason, this paper presents a reaction-free control strategy and associated complete dynamic modeling in order to reduce the bearing friction and thus to improve the system performance of the VR spherical motor.

This paper derives an analytical model describing the resultant magnetic force to serve as a basis for designing the reaction-free control strategy. The paper presents a practical technique for approximating experimentally the permeance, which plays an important role in modeling and hence the development of the control law, without changing the previous experimental setup. Preliminary experimental results show that the reaction-free control strategy reduces the bearing friction and improves the system performance. Several system performance evaluation techniques are also addressed in the paper. It is expected that the complete dynamic modeling and the reaction-free control strategy will serve as a basis for modeling and control of six DOF VR spherical motors with contact or non-contact support mechanism.

1. INTRODUCTION

A VR spherical motor with a contact transfer bearing support mechanism has been discussed by Lee *et al.* in 1993. Although the unmodeled resultant magnetic force can be balanced by the bearing support system, the reaction on the bearings generates significant friction and bearing noise in the control of the motor at high frequencies. For precision applications of the VR spherical motor, it is desired that the magnetic force be self-balanced, in other words, the rotor be self magnetically levitated, so that the reactions exerted by the transfer bearings are negligible. The design of the VR spherical motor with redundant actuation (excitation) provides such a possibility of a reaction-free self magnetically levitated mechanism without complicating the structure and the control of the overall system. Balancing the magnetic force, however, requires an explicit modeling of the magnetic force and a reaction-free control strategy. This paper presents a reaction-free control strategy, the associated complete dynamic modeling, and several system performance evaluation techniques.

The structure of the VR spherical motor used in this paper is similar to that described by Lee *et al.* (1993a). However, the idea and approach toward the modeling and control of the device is different from the ones in previous research. This paper presents first a complete set of dynamic models including the derivation of magnetic force expression. The paper then proposes a reaction-free control strategy which will self-balance the magnetic force by choosing properly the electrical inputs through the stator coils. Results of the experiments validating the control strategy and the magnetic force model are presented with emphasis placed on the force tests. Several system performance evaluation techniques are also addressed in the paper to facilitate the experiments.

The main contributions of this paper are summarized as follows. (1) A reaction-free control strategy is proposed so that the rotor can be self magnetically levitated without complicating the structure and control of the present VR spherical motor. The elimination of the bearing friction by the magnetic levitation offers precision motion control and fast dynamic response.

(2) The resultant magnetic force is explicitly modeled, which completes the dynamic modeling of the electromagnetic interaction of the VR spherical motor prototype. (3) The explicit expression of the bearing friction is given based on the analytical magnetic force model. The friction model can be used to evaluate the torque discrepancies and to predict the net mechanical torque output.

The rest of the paper consists of four sections. Section 2 derives the magnetic model and summarizes the complete set of dynamic models. Section 3 proposes the reaction-free control strategy based on the analytical dynamic model in order to reduce the bearing friction thus to improve the system performance. Section 4 presents experimental methods for approximating the permeance function with variable airgap, for analyzing the bearing friction, and for calculating the net mechanical torque output of the VR spherical motor. Also Section 4 discusses some preliminary experimental results. Finally, Section 5 draws some basic conclusions.

2. A COMPLETE SET OF DYNAMIC MODELS

The elimination of the bearing friction by magnetic levitation requires an explicit modeling of the magnetic force. The modeling of the magnetic torque has been discussed by Lee *et al.* (1993a). This section presents the modeling of the magnetic force and summarizes the complete dynamic models.

2.1 Rotational / Translational Dynamics

The rotor of the VR spherical motor prototype is a typical single-body mechanical system with six degrees of freedom. In terms of Z-Y-Z Euler angles, $\mathbf{q}_T = [\psi, \theta, \phi]^T$, and the linear displacement of the center of the rotor, $\mathbf{q}_F = [X_1, X_2, X_3]^T$, the rotor dynamic equations are given as follows:

$$\mathbf{M}_T(\mathbf{q}_T)\ddot{\mathbf{q}}_T + \mathbf{h}_T(\mathbf{q}_T, \dot{\mathbf{q}}_T) = \mathbf{T}, \tag{1}$$

$$\mathbf{M}_F\ddot{\mathbf{q}}_F = \mathbf{F}, \tag{2}$$

where $\mathbf{M}_T(\mathbf{q}_T) = \begin{bmatrix} -IS_\theta C_\phi & IS_\phi & 0 \\ IS_\theta C_\phi & IC_\phi & 0 \\ I_z C_\theta & 0 & I_z \end{bmatrix},$

$$\mathbf{M}_F = \begin{bmatrix} m_r & 0 & 0 \\ 0 & m_r & 0 \\ 0 & 0 & m_r \end{bmatrix},$$

$$\mathbf{h}_T(\mathbf{q}_T, \dot{\mathbf{q}}_T) = \begin{bmatrix} I(-\dot{\psi}\dot{\theta}C_\theta C_\phi + \dot{\psi}\dot{\phi}S_\theta S_\phi + \dot{\theta}\dot{\phi}C_\phi) - (I - I_z)(\dot{\psi}S_\theta S_\psi + \dot{\theta}C_\phi)(\dot{\psi}C_\theta + \dot{\phi}) \\ I(\dot{\psi}\dot{\theta}C_\theta S_\phi + \dot{\psi}\dot{\phi}S_\theta C_\phi - \dot{\theta}\dot{\phi}S_\phi) - (I_z - I)(-\dot{\psi}S_\theta C_\phi + \dot{\theta}S_\phi)(\dot{\psi}C_\theta + \dot{\phi}) \\ -I_z\dot{\psi}\dot{\theta}S_\theta - 0 \end{bmatrix}$$

and where $\mathbf{T} = [T_1, T_2, T_3]^T$ is the actuating torque about the center of the rotor with respect to the rotor body frame; $\mathbf{F} = [F_1, F_2, F_3]^T$ is the resultant force passing through the center of the rotor expressed in the stator fixed coordinate frame; m_r is the mass of the rotor, $I = I_x = I_y$ and I_z are the moments of inertia about the principle axes; and $S_{(\bullet)}$ and $C_{(\bullet)}$ denote the trigonometric sine and cosine functions of the angle $(\bullet)$, respectively.

2.2 Magnetic Torque Generation and the Resultant Magnetic Force

The VR spherical motor has been extended conceptually from three DOF to six DOF by allowing the rotor to translate. This extension provides a "virtual-work-like" method to model analytically the magnetic force, which will be discussed in the following. The torque and force generated by the electromagnetic system are governed by the principle of conservation of energy. If the heat dissipation is neglected, the principle of conservation of energy states that

$$\dot{E}_e(t) - \dot{E}_m(t) = \vec{T}(t) \bullet \vec{\omega}(t) + \vec{F}(t) \bullet \vec{v}(t) + m_r g\dot{X}_3 \tag{3}$$

where $\dot{E}_m$ is the time rate of magnetic energy stored in the airgap; $\dot{E}_e$ is the electrical power input; $\vec{\omega}$ is the angular velocity of the rotor; $\vec{v}$ is the linear velocity of the center of the rotor; and g is the acceleration due to gravity. The rotational and translational mechanical powers can be rewritten as

$$\vec{T} \bullet \vec{\omega} = \sum_{k=1}^{3} T_k\dot{\phi}_k, \tag{4}$$

$$\vec{F} \bullet \vec{v} = \sum_{k=1}^{3} F_k\dot{X}_k \tag{5}$$

where the time derivatives of ϕ_k are the angular velocity components measured with respect to the rotor body frame; and the time derivatives of X_k are the linear velocity components along X, Y, Z axes of the stator fixed frame. Since $\vec{F}$ is the resultant (equivalent) force through the center of the rotor, it has no effect on the magnetic torque generation. In addition, noting that ϕ_k and X_k are independent of each other, the torque generated by the electromagnetic system is then given by

$$\vec{T}_m \stackrel{\Delta}{=} \vec{T} = \nabla_T(E_e - E_m) \tag{6}$$

where $\nabla_T = \left(\dfrac{\partial}{\partial\phi_1}\right)\vec{c}_1 + \left(\dfrac{\partial}{\partial\phi_2}\right)\vec{c}_2 + \left(\dfrac{\partial}{\partial\phi_3}\right)\vec{c}_3$

and $\vec{c}_k (k = 1, 2, 3)$ is the unit vector along the axis of the rotor body frame. The resultant magnetic force is governed by

$$\vec{F}_m \stackrel{\Delta}{=} \vec{F} + m_r g\vec{E}_3 = \nabla_F(E_e - E_m) \tag{7}$$

where $\nabla_F = \left(\dfrac{\partial}{\partial X_1}\right)\vec{E}_1 + \left(\dfrac{\partial}{\partial X_2}\right)\vec{E}_2 + \left(\dfrac{\partial}{\partial X_3}\right)\vec{E}_3,$

and $\vec{E}_k (k = 1, 2, 3)$ is the unit vector along the axis of the stator fixed frame.

It has been derived by Lee *et al.* (1993a) that

$$\dot{E}_e - \dot{E}_m = \frac{1}{2}\sum_{i=1}^{m}\sum_{j=1}^{n}(M_{si} + M_{rj} - V)^2\dot{P}_{ij}$$

where M_{si} and M_{rj} denote the magnetomotive forces (mmf's) generated by the i^{th} stator pole and the j^{th} rotor pole respectively;

and V represents the magnetic potential of the magnetic conductor layer at the stator shell with respect to that at the center of the rotor. Using this relationship in Equations (6) and (7), the magnetic torque and force are expressed in terms of the mmf's and permeance function as

$$\vec{T}_m = \frac{1}{2}\sum_{i=1}^{m}\sum_{j=1}^{n}(M_{si} + M_{rj} - V)^2 \nabla_T P_{ij}, \tag{8}$$

and

$$\vec{F}_m = \frac{1}{2}\sum_{i=1}^{m}\sum_{j=1}^{n}(M_{si} + M_{rj} - V)^2 \nabla_F P_{ij}. \tag{9}$$

2.3 Permeance Function with Variable Airgap

As shown in Equations (8) and (9), the magnetic torque and force models depend on the permeance function, P_{ij}. This section investigates the geometric variables and their relationships used in determining the permeance function.

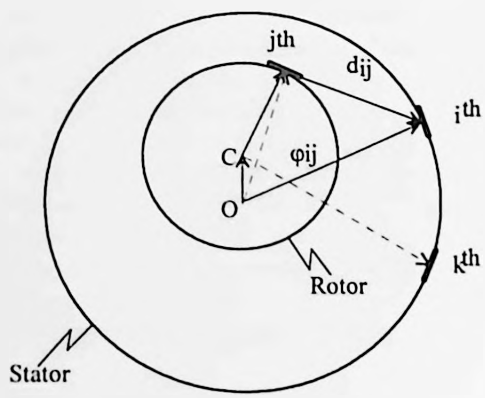

FIG. 1 INDEPENDENT GEOMETRIC VARIABLES OF THE PERMEANCE MODEL AND THEIR RELATIONSHIPS

Unlike the three DOF case (Lee *et al.*, 1993b), the center of the rotor of the six DOF VR spherical motor is allowed to move; therefore, the permeance P_{ij} is a function of the relative position between the stator poles and the rotor poles. The relative position is described by the angle between the position vectors of the i^{th} stator pole and the j^{th} rotor pole and by the distance between the i^{th} stator pole and the j^{th} rotor pole, namely, $P_{ij} = P(\varphi_{ij}, d_{ij})$. Fig. 1 is a two dimensional projection of the three dimensional structure of the VR spherical motor, which depicts the geometric relationship of the vectors representing the angle and the distance. The angle, φ_{ij}, can be determined from the dot product of the position vectors of the i^{th} stator pole and j^{th} rotor poles with respect to the stator frame as follows:

$$\cos(\varphi_{ij}) = \frac{\vec{O}_{si} \bullet \vec{O}_{rj}}{R\left\|\vec{O}_{rj}\right\|}$$

where $\vec{O}_{rj} = \vec{O}_c + \vec{C}_{rj} = \left\|\vec{O}_c\right\|\vec{e}_c + r\vec{e}_{rj}$; R and r are the radii of the stator shell and rotor sphere respectively; and $\vec{O}_{si}$ and $\vec{O}_{rj}$ are the position vectors of the i^{th} stator pole and the j^{th} rotor pole, respectively. Also, since $\vec{D}_{ij} = \vec{O}_{si} - \vec{O}_{rj}$, the distance between the i^{th} stator pole and j^{th} rotor pole can be calculated from the following vector dot product:

$$d_{ij} = \left(\vec{D}_{ij} \bullet \vec{D}_{ij}\right)^{\frac{1}{2}} = \left[\left(\vec{O}_{si} - \vec{O}_{rj}\right) \bullet \left(\vec{O}_{si} - \vec{O}_{rj}\right)\right]^{\frac{1}{2}}.$$

From Equations (8) and (9), it has been shown (Lee *et al.*, 1993a) by using differential geometry that the magnetic torque is given by

$$\vec{T}_m = \frac{1}{2}\sum_{i=1}^{m}\sum_{j=1}^{n}\left[(M_{si} + M_{rj} - V)^2 \left.\frac{\partial P(\varphi, d_{ij})}{\partial \varphi}\right|_{\varphi=\varphi_{ij}} \vec{e}_{ij}\right] \tag{10}$$

where $\vec{e}_{ij}$ is the unit vector perpendicular to the position vectors $\vec{O}_{si}$ and $\vec{O}_{rj}$. The unit vector can be determined from the following vector cross product:

$$\vec{e}_{ij} = \frac{\vec{O}_{si} \times \vec{O}_{rj}}{\left\|\vec{O}_{si}\right\|\left\|\vec{O}_{rj}\right\| \sin(\varphi_{ij})}. \tag{11}$$

By a similar derivation on Equation (7), it can be shown that the resultant force is given by

$$\vec{F}_m = \frac{1}{2}\sum_{i=1}^{m}\sum_{j=1}^{n}\left[(M_{si} + M_{rj} - V)^2 \left.\frac{\partial P(\varphi_{ij}, d)}{\partial d}\right|_{d=d_{ij}} \vec{e}'_{ij}\right] \tag{12}$$

where the unit vector $\vec{e}'_{ij}$ is along the straight line connecting the stator and rotor poles; and it is given by

$$\vec{e}'_{ij} = \vec{D}_{ij} / \left(\vec{D}_{ij} \bullet \vec{D}_{ij}\right)^{\frac{1}{2}}.$$

The permeance function, $P(\varphi_{ij}, d_{ij})$, will be determined experimentally.

2.4 Quadratic Representation of the Torque and Force Models

Consider a specific configuration where only simple iron cores are used as rotor poles (i.e., $M_{rj} = 0, j = 1, ..., n$). Suppose current sources are used as excitations and the mmf's of the stator coils are treated as system inputs, then the generated torque and the resultant force given by Equations (10) and (12) can be written in matrix form as follows:

$$T_{m\iota} = \frac{1}{2}\mathbf{u}^T A_\iota \mathbf{u}, \tag{13}$$

$$F_{m\iota} = \frac{1}{2}\mathbf{u}^T \mathbf{B}_\iota \mathbf{u} \tag{14}$$

where $\iota = 1, 2, 3$

$$\mathbf{u} = [M_{s1}, M_{s2}, ..., M_{sm}]^T \in \mathbf{R}^m,$$

$$\mathbf{A}_\iota = \sum_{i=1}^{m}\left(\sum_{j=1}^{n}\left.\frac{\partial P(\phi, d_{ij})}{\partial \phi}\right|_{\phi=\phi_{ij}} (\vec{e}_{ij} \bullet \vec{e}_\iota)\right)(\mathbf{a} - \mathbf{c}_i)(\mathbf{a} - \mathbf{c}_i)^T, \tag{15}$$

$$\mathbf{B}_\iota = \sum_{i=1}^{m}\left(\sum_{j=1}^{n}\left.\frac{\partial P(\phi_{ij}, d)}{\partial d}\right|_{d=d_{ij}} (\vec{e}'_{ij} \bullet \vec{E}_\iota)\right)(\mathbf{a} - \mathbf{c}_i)(\mathbf{a} - \mathbf{c}_i)^T, \tag{16}$$

$$\mathbf{c}_i = [0, ...0, \underset{i^{th}}{1}, 0, ..., 0]^T,$$

$$\mathbf{a} = [a_1, a_2, ..., a_i, ..., a_m]^T,$$

$$a_i = \sum_{j=1}^{n} P_{ij} / (\sum_{i=1}^{m} \sum_{j=1}^{n} P_{ij}) \quad \text{and} \quad \sum_{i=1}^{m} a_i = 1$$

and where the matrices $\mathbf{A}_\iota$ and $\mathbf{B}_\iota$ ($\iota = 1,2,3$) are functions of both orientation and translation of the rotor.

3. REACTION-FREE MOTION CONTROL STRATEGY

The objective of reaction-free control strategy is to control (balance) the resultant force, while generating the required torque for a desired rotation, so that the rotor is magnetically levitated rendering the friction between the rotor and the bearings negligible. Due to the elimination of the friction, the VR spherical motor with reaction-free control strategy will have a high-precision torque control, a smooth motion, and a fast dynamic response.

3.1 Reaction-free Torque/Force Control Strategy

The torque and force required to generate a specified trajectory are referred as the torque/force control laws. The desired trajectory (path) is specified as

$$q_d = [q_{dT}^T, q_{dF}^T]^T = [\psi, \theta, \phi, 0, 0, 0]^T$$

where the Euler angles, ψ, θ, and ϕ, are functions of time. From Equation (2), the force control law $\mathbf{F} = \mathbf{M}_F \ddot{\mathbf{q}}_{dF}$ will guarantee that the linear displacement tracking error approaches to zero asymptotically. Since $\mathbf{q}_{dF} = \mathbf{0}$, the reaction-free force control law is determined by

$$F_1 = 0, \qquad\qquad F_{m1} = 0,$$

$$F_2 = 0, \qquad \text{or} \qquad F_{m2} = 0,$$

$$F_3 = 0 \qquad\qquad F_{m3} = m_r g$$

where the magnetic force component in Z direction will balance (compensate) the gravity of the rotor.

The torque control law can be designed by using the computed torque method or Lyapunov method (Lee *et al.*, 1993a).

3.2 Solution to the Inverse Magnetics

The inverse magnetics are defined here as to find the electrical inputs through the stator coils which would generate the required magnetic force and torque determined from the reaction-free control strategy.

Other than the three torque constraints from the torque control law (Lee *et al.*, 1993a), the following three force constraints are added to the optimization formulation for solving uniquely the inverse magnetics:

$$\frac{1}{2}\mathbf{u}^T\mathbf{B}_1\mathbf{u} = 0,$$

$$\frac{1}{2}\mathbf{u}^T\mathbf{B}_2\mathbf{u} = 0,$$

$$\frac{1}{2}\mathbf{u}^T\mathbf{B}_3\mathbf{u} = m_r g.$$

In practical implementation of the optimization algorithm, the torque and force constraints are combined via penalty (weighting) factors with the objective function such as the consumed electrical power. Different penalty factors can be used as the weights of the torque and force errors to specify the different priority on the corresponding torque and force constraints.

4. EXPERIMENTAL INVESTIGATION

The experimental testbed used to verify the analytical magnetic force model and to validate the reaction-free control strategy is similar to that described by Roth *et al.* (1993), except that all the stator coils are assembled this time. In addition, the rotor is allowed to translate; in other words, the motor has six degrees of freedom. However, only the three DOF rotation are used in motion realization. The three DOF translation are used to levitate and center the rotor for non-contact magnetic support of the mechanism.

4.1 Experimental Approximation of the Permeance

The accurate experimental determination of the permeance requires knowledge of the displacement of the rotor, which is relatively difficult to measure in practice. Therefore, it is preferable that the permeance be approximated using the experimental permeance model derived based on the orientation variables only (Roth *et al.*, 1993). Since the displacement (translation) of the center of the rotor is small compared to the radii of the rotor and stator, the centers and the poles of the rotor and the stator form approximately a triangle as shown in Fig. 1. By cosine law, we have

$$d^2 \approx R^2 + r^2 - 2Rr\cos\varphi \approx 2\bar{R}^2(1 - \cos\varphi) \tag{17}$$

or

$$\cos\varphi \approx 1 - d^2/(2\bar{R}^2) \tag{18}$$

where $\bar{R}$ is the mean radius of the sphere separating the rotor and stator poles. By taking the derivative with respect to the variable d on both sides of Equation (18) and using Equation (17), we obtain

$$\frac{\partial\varphi}{\partial d} = \frac{d}{\bar{R}^2 \sin\varphi} = \frac{[2(1-\cos\varphi)]^{\frac{1}{2}}}{\bar{R}\sin\varphi} \qquad (\varphi \neq 0).$$

Using the chain rule of derivative, the partial derivative of the permeance with respect to the variable d can be approximated in terms of full derivative with respect to the variable φ and the angle itself as

$$\frac{\partial P(\varphi, d)}{\partial d} = \frac{dP(\varphi)}{d\varphi} \frac{[2(1-\cos\varphi)]^{\frac{1}{2}}}{\bar{R}\sin\varphi} \tag{19}$$

where the $P(\varphi)$ is the permeance function derived experimentally based on rotor orientations only.

In the vicinity of the origin, $\varphi = 0$, in other words, when the stator and rotor pole pair is fully overlapped, Equation (19) is no longer valid. In this case, it has been shown (Pei, 1990) that

$$P(\varphi, d) = \frac{\mu_0[2\pi r(1 - \cos\varphi_{min})]}{d};$$

therefore, $\frac{\partial P}{\partial d} = -\frac{\mu_0[2\pi r(1-\cos\varphi_{min})]}{d^2}$

where μ_0 is the permeability of air; $d = R - r$ corresponds the airgap length; and $\varphi_{min} = 16°$ for the prototype VR spherical motor. Once $\partial P/\partial d$ is known, $\mathbf{B}_\iota$ thus $F_{m\iota}$ (ι = 1, 2, 3) can be calculated from Equations (16) and (14).

4.2 Bearing Friction Analysis

Previous torque test experiments showed that the transfer bearing friction of the prototype VR spherical motor is significant especially for small torque output at low speed. The bearing friction contributes to the torque error in modeling; and therefore degrades the control system performance. The friction force/torque is directly proportional to the normal component of the magnetic force generated by the electromagnetic system. To account the friction effect on the torque output, the friction force can be modeled explicitly based on Equation (7) and the analytical magnetic force expression, Equation (12). The results are shown as follows:

$$\vec{f} = \left(\sum_{k=1}^{m_b} \vec{F} \bullet \vec{C}_{bk}\right)\alpha\vec{e}_f \tag{20}$$

where $\vec{C}_{bk}$, as shown in Fig. 1, is the coordinate (position) vector of the k^{th} bearing with respect to the rotor frame and $\vec{C}_{bk} = \vec{O}_c + \vec{O}_{bk}$; α is the friction coefficient between the bearings and the rotor; m_b is the number of bearings; and $\vec{e}_f$ is the unit vector in the opposite direction of the instantaneous velocity of the contact point on the rotor, and it is given by

$$\vec{e}_f = -\frac{\vec{\omega}\times\vec{C}_{bk}}{\left\|\vec{\omega}\times\vec{C}_{bk}\right\|}.$$

4.3 Net Mechanical Torque Output

The net mechanical torque output, the data obtained using an F/T sensor, is in fact the difference between the magnetic and the friction torques, namely,

$$\vec{T} = \vec{T}_m - \vec{\tau}_f$$

where $\vec{\tau}_f$ denotes the torque caused by the friction, and $\vec{\tau}_f = \vec{C}_{bk}\times\vec{f}$. Therefore,

$$\vec{T} = \vec{T}_m - \vec{C}_{bk}\times\left(\sum_{k=1}^{m_b}\vec{F}\bullet\vec{C}_{bk}\right)\alpha\vec{e}_f. \tag{21}$$

Ideally, the magnetic force is self-balanced if the reaction-free force control law, $\mathbf{F} = \mathbf{0}$, is used. In this case, the net mechanical torque output is equal to the magnetic torque generated.

4.4 Preliminary Experimental Results and Discussions

Theoretical analysis shows that the torque discrepancies between the actual and model-predicted torques can be reduced if the reaction-free control strategy is used in the motion control of the VR spherical motor. For comparison with the three DOF case where the unmodeled magnetic force was balanced by the transfer bearings, a number of torque/force tests at rotor orientation (0°, 0°, 0°) have been performed. TABLEs 1 and 2 list the torque and force measurements with various specified torques in z direction in cases with or without the force model, respectively. The magnitude of the desired torques was limited in the experiments to be less than 0.1 Nm in order to avoid the magnetic saturation of the magnetic circuit, which is another factor contributing to the torque discrepancies. One observes from the last three columns of TABLEs 1 and 2 that the overall resultant force acting on the rotor, particularly the force component in Z direction, is reduced when the magnetic force model is taken into consideration in the motion control of the motor. Also listed in the TABLEs are the torque differences between the desired and the actual torque values. As shown in Fig. 2, within the range of desired/actual torque less than 0.1 Nm, the torque errors accounting for the effect of the force model are, in general, smaller or in the same order of magnitude than that of the case without the force model within the measurement tolerance of the F/T sensor. The improvement of the torque error of using the force model is expected to be more significant for torque tests with larger desired torque, because of the more significant reduction of the magnetic force. Since the resultant force with the

TABLE 1 EXPERIMENTAL TORQUE/FORCE DATA WITHOUT THE FORCE MODEL

T_{d3}	T_3	$T_{d3}-T_3$	F_1	F_2	F_3
-0.08	-0.0726	-0.0074	0.0945	-0.0167	2.9247
-0.06	-0.0484	-0.0116	0.1223	0.0056	0.2502
-0.04	-0.0441	0.0041	0.0945	0.0000	1.2399
-0.02	-0.0169	-0.0031	0.0334	0.0111	0.0445
0.00	-0.0001	0.0001	0.0056	0.0111	-0.0000
0.02	0.0237	-0.0037	0.0612	0.0000	0.4893
0.04	0.0456	-0.0056	0.1168	-0.0222	1.1621
0.06	0.0532	0.0068	0.1112	0.0000	-0.1501
0.08	0.0862	-0.0062	0.2002	-0.0334	2.6856

Force in N, and Torque in Nm.

TABLE 2 EXPERIMENTAL TORQUE/FORCE DATA WITH THE FORCE MODEL

T_{d3}	T_3	$T_{d3}-T_3$	F_1	F_2	F_3
-0.08	-0.0665	-0.0135	-0.4993	0.3905	-0.5284
-0.06	-0.0549	-0.0051	-0.0890	0.1186	-0.3035
-0.04	-0.0287	-0.0113	-0.3392	0.1890	-0.2335
-0.02	-0.0147	-0.0053	-0.1724	0.1668	-0.0500
0.00	-0.0000	0.0000	0.0000	-0.0056	0.0000
0.02	0.0240	-0.0040	-0.0371	0.0369	-0.3013
0.04	0.0452	-0.0052	-0.1890	-0.2502	-0.7673
0.06	0.0596	0.0004	-0.0982	-0.0760	-1.5402
0.08	0.0859	-0.0059	-0.2502	-0.4504	-1.4846

Force in N, and Torque in Nm.

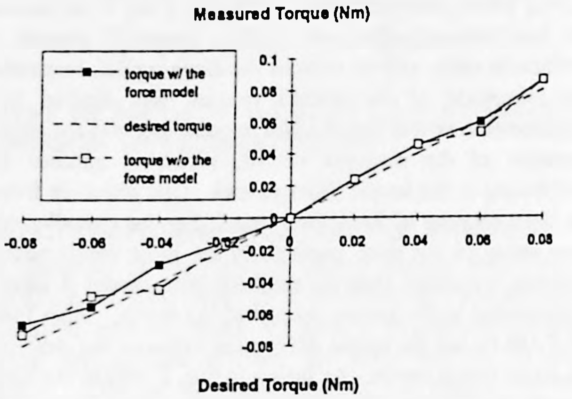

FIG. 2 TORQUE ERRORS WITH AND WITHOUT THE FORCE MODEL

reaction-free control strategy is relatively small compared to the three DOF case, the uncertainty in measuring the torque components in x and y directions using the experimental setup (Roth, 1992) will be reduced more significantly than that in z direction.

It is worth noting that to evaluate the effect of bearing friction on the torque output, bearing friction and net mechanical torque output can be computed using Equations (20) and (21) based on the torque/force experimental data listed in the TABLEs.

5. CONCLUSIONS

The VR spherical motor has been extended conceptually from three DOF to six DOF. The translational degrees of freedom have been used creatively to design a reaction-free control strategy based on a complete dynamic modeling without any hardware reconstruction. A "virtual-work-like" energy-based method has been used to derive explicitly the magnetic force model which is vital in high-precision torque control and which had never been explored in the previous VR spherical motor research. The reaction-free control strategy enables the VR spherical motor to be self magnetically levitated, so that the bearing friction is reduced and the system performance is improved. The associated system performance evaluation techniques presented in this paper provide a means to analyze quantitatively the effect of the bearing friction. Preliminary experimental results at rotor orientation (0°, 0°, 0°) showed a reasonably good agreement with the theoretical analysis. The torque/force test experiments at other rotor orientations throughout the entire workspace are currently been investigated.

ACKNOWLEDGMENT

This work is supported by the National Science Foundation under the grant number DDM-8958383.

REFERENCES

Lee, K-M, Wang, Xiao-an, Wang, Nanhua, 1993, "Dynamic Modeling and Control of a Ball-joint-like Variable-reluctance Spherical Motor," *Symposium on Mechatronics*, ASME Winter Annual Meeting, November, 1993, New Orleans, LA, pp. 71-79.

Lee, K-M, Zhou, Zhi, and Wang, Nanhua, 1993, "A Practical Optimal Control Strategy for a Variable Reluctance Spherical Motor," *Symposium on Mechatronics*, ASME Winter Annual Meeting, November, 1993, New Orleans, LA, pp. 39-47.

Lee, K-M., 1992, "Development of a Spherical Wrist Motor," National Science Foundation Conference Video Preview, Atlanta, GA, Black#95-102.

Pei, J., 1990, "Methodology of Design and Analysis of Variable-Reluctance Spherical Motor," *Ph.D. Thesis*, Mechanical Engineering, Georgia Institute of Technology, Atlanta, GA.

Roth, Ronald. B, 1992, *An Experimental Investigation and Optimization of a Variable Reluctance Spherical Motor*, Ph. D. Thesis, Mechanical Engineering, Georgia Tech, Atlanta, GA.